Cell Biology:

DEF6, a Novel Substrate for the Tec Kinase ITK, Contains a Glutamine-rich Aggregation-prone Region and Forms Cytoplasmic Granules that Co-localize with P-bodies

Fiona Hey, Nathan Czyzewicz, Peter Jones
and Fred Sablitzky

J. Biol. Chem. 2012, 287:31073-31084.
doi: 10.1074/jbc.M112.346767 originally published online July 24, 2012

THE JOURNAL OF BIOLOGICAL CHEMISTRY VOL. 287, NO. 37, pp. 31073–31084, September 7, 2012

DEF6, a Novel Substrate for the Tec Kinase ITK, Contains a Glutamine-rich Aggregation-prone Region and Forms Cytoplasmic Granules that Co-localize with P-bodies*[S]

Received for publication, January 26, 2012, and in revised form, July 12, 2012 Published, JBC Papers in Press, July 24, 2012, DOI 10.1074/jbc.M112.346767

Fiona Hey[‡1], **Nathan Czyzewicz**[‡], **Peter Jones**[§2], **and Fred Sablitzky**[‡2,3]

From the [‡]*School of Biology, Molecular Cell and Developmental Biology and the* [§]*School of Biomedical Sciences, The University of Nottingham, Nottingham NG7 2UH, United Kingdom*

Background: DEF6 is recruited to the immunological synapse upon T cell receptor-mediated signaling regulating inflammatory responses including Experimental Autoimmune Encephalomyelitis.
Results: DEF6 is a substrate for ITK and forms granules co-localizing with P-bodies.
Conclusion: DEF6 granule formation is likely to be mediated by unmasking a Q-rich coiled-coil region in the C terminus.
Significance: Discovery of a potential link between T cell receptor-mediated signaling and translation regulation in P-bodies.

Localization of DEF6 (SLAT/IBP), a Rho-family guanine nucleotide exchange factor, to the center of the immune synapse is dependent upon ITK, a Tec-family kinase that regulates the spatiotemporal organization of components of T cell signaling pathways and Cdc42-dependent actin polymerization. Here we demonstrate that ITK both interacts with DEF6 and phosphorylates DEF6 at tyrosine residues Tyr^{210} and Tyr^{222}. Expression of a GFP-tagged Y210E-Y222E phosphomimic resulted in the formation of DEF6 cytoplasmic granules that co-localized with decapping enzyme 1 (DCP1), a marker of P-bodies; sites of mRNA degradation. Similarly treatment of cells with puromycin or sodium arsenite, reagents that arrest translation, also resulted in the accumulation of DEF6 in cytoplasmic granules. Bioinformatics analysis identified a glutamine-rich, heptad-repeat region; a feature of aggregating proteins, within the C-terminal region of DEF6 with the potential to promote granule formation through a phosphorylation-dependent unmasking of this region. These data suggest that in addition to its role as a GEF, DEF6 may also function in regulating mRNA translation.

DEF6 (1, 2) also described as SLAT (3) or IBP (4), is a 631 amino acid Rho-family guanine nucleotide exchange factor (GEF)[4] that is highly expressed in mature T cells. It is one of a complement of signaling molecules that function downstream of the T cell receptor at the immune synapse, a junction between T cells and antigen presenting cells, where it has been identified to play a role in coordinating actin cytoskeleton remodeling, and Ca^{2+} and NFAT signaling (5, 6). Inactivation of DEF6 expression by retroviral insertion in transgenic mice has also identified a role for DEF6 in regulating the expression of the inflammatory interleukin IL-17 (7, 8), although whether DEF6 acts as a positive or negative regulator remains to be clarified. In contrast with Vav1, the best-characterized Rho GEF in T cells (9), relatively little is known about the extent of the roles of DEF6, its regulation or how its structure relates to its function. Based upon limited homology with other Rho-family GEFs, DEF6 can be divided into four modular domains. The N terminus contains two putative calcium-binding EF hands followed by a DSH domain (DEF6-SWAP-70 homology, amino acids 73–216) of unknown function that contains a putative ITAM motif (5), a pleckstrin homology (PH) domain (amino acids 217–312) and a C-terminal Dbl homology-like (DHL) domain (2). DEF6 is atypical as the N-C-terminal organization of the PH and DHL domains, hallmarks of Rho-family GEFs, is reversed; a feature shared with the only relative of DEF6, the Rho GEF SWAP-70 that is expressed predominantly in B cells (10). Roles have been attributed to the PH domain, which binds preferentially to phosphatidyl inositol 3,4,5-trisphosphate (11) and the DHL domain responsible for nucleotide exchange activity (2, 11). In addition, the tyrosine kinase LCK has been identified as a regulator of DEF6 function. Phosphorylation by LCK has been found to be necessary for recruitment of DEF6 to the immune synapse (11). Initial studies identified tyrosine 210 of DEF6 as the residue phosphorylated by LCK (11) but subsequently tyrosines 133 and 144 were shown to be LCK targets (5). However, the dynamic structure of the immune synapse is regulated extensively through the activity of different families of kinase other than LCK including the Syk-family kinase ZAP-70 and the Tec-family kinase, ITK (12–14), and given that ITK-deficient mice exhibited a very similar phenotype to the DEF6-deficent mice (7, 8, 15), we explored the possibility that, in addition to LCK, DEF6 might be a substrate of ITK. ITK is a member of the Tec-family of tyrosine kinases that regulate lymphocyte development, activation and differentiation. ITK consists of an N-terminal PH domain followed by a Zn^{2+}-binding region (BH motif), a proline-rich region (PRR), and an SH_3-SH_2-kinase domain cassette found in Src and Csk kinases (12). In response to TCR activation and the generation of phosphatidyl (3, 4, 5)

* This work was supported through the University of Nottingham and a MRC studentship (to F. H.).
[S] This article contains supplemental Figs. S1 and S2.
[1] Present address: University of Leicester, UK.
[2] Both authors contributed equally to this work.
[3] To whom correspondence should be addressed: The University of Nottingham, Molecular Cell and Developmental Biology, Queen's Medical Centre, Nottingham NG7 2UH, UK. Tel.: 0044-115-82-30324; Fax: 0044-115-82-30338; E-mail: fred.sablitzky@nottingham.ac.uk.
[4] The abbreviations used are: GEF, guanine nucleotide exchange factor; FL, full-length; aa, amino acids; KD, kinase dead.

trisphosphate, ITK is recruited to the membrane where it interacts with the phosphorylated SLP76/LAT complex via its SH2 and SH3 domains. Here it is phosphorylated by LCK at tyrosine 511 in the activation loop of its kinase domain and is autophosphorylated at tyrosine 180 within its SH3 domain (16, 17). Activation of ITK subsequently results in increased intracellular Ca^{2+} and diacylglycerol concentrations through tyrosine-phosphorylation and activation of its substrate PLCγ and as we show here, phosphorylation of amino acid residues Tyr^{210} and Tyr^{222} of DEF6. Our data provide a biochemical link to the recently described phenomenon that the spatiotemporal organization of cdc42 and DEF6 is ITK-dependent. ITK selectively recruits DEF6 to the center of the interface between the T cell and antigen presenting cell (18). In addition, we demonstrate that a mutant of DEF6 (Y210E-Y222E) that mimics its phosphorylation by ITK causes it to assemble into cytoplasmic granules that are similar in appearance to stress granules and/or mRNA processing bodies (P-bodies); structures involved in the regulation of mRNA translation (19, 20). As is the case for formation of stress granules and P-bodies, wild-type DEF6 can also be induced to form cytoplasmic granules by cell stress through treatment with either sodium arsenite or puromycin (21). Indeed, we demonstrate that wild-type and Y210E-Y222E mutant of DEF6 co-localize with the P-body marker DCP1 under cellular stress in COS-7 cells and in Jurkat cells treated with the phosphatase inhibitor pervanadate. Furthermore, in contrast to wild-type DEF6 that upon TCR-mediated signaling is evenly distributed in the immunological synapse, co-localizing with f-actin, the Y210E-Y222E mutant of DEF6 aggregates and does not appear to co-localize with f-actin. We propose that phosphorylation of DEF6 by ITK, or cellular stress, regulates a switch in the conformation of DEF6 facilitating aggregation by unmasking a glutamine-rich coiled-coil region in the DHL domain (22) resulting in P-body localization.

EXPERIMENTAL PROCEDURES

Antibodies—Monoclonal GFP (G1546) and β-actin (A1978) antibodies were purchased from Sigma. Polyclonal GFP antibody used for immunoprecipitations was kindly provided by Dr Sally Wheatley and the polyclonal GST antibody used for immunoblotting was kindly provided by Dr Simon Dawson (both Department of Biochemistry, The University of Nottingham). Monoclonal ITK antibody (Ab3302) was purchased from Abcam (Cambridge, MA) and PY20 (610000) from BD Transduction Labs (San Jose, CA). Rabbit α-DEF6 antisera (raised against aa 410–630 of DEF6) (23) was kindly provided by Dr. Thomas Samson (Department of Cell and Developmental Biology, University of North Carolina). Alexafluor rabbit 568 (A11036) was from Molecular Probes, Invitrogen.

Recombinant Proteins—DEF6 full-length (1–631) as well as PH-DHL (105–631), PH^1 (207–330), PH^2 (214–341), and DHL (355–631) domains were amplified and subcloned into the appropriate pEGFP-C vectors (Invitrogen). In-frame cloning and integrity was verified by sequencing. DEF6 tyrosine to glutamate or to phenylalanine mutants were generated by using Quickchange Mutagenesis (Stratagene). pEGFP-N1-ITK and pEGFP-N1-ITK-KD are of mouse origin and were kindly provided by Dr. P. Schwartzberg (National Human Genome Research Institute, National Institutes of Health, Bethesda, MD). Both, wild-type ITK (ITK WT) and kinase-dead ITK (ITK KD) were subsequently subcloned into DsRed-Express-N1 (Clontech) and constructs verified by sequencing. The DsRed-tagged DCP1b construct was kindly provided by Y. Shav-Tal (Bar Ilan University, Israel).

To produce a His-tagged full-length human DEF6 protein, *Spodoptera frugiperda* 9 cells were infected with a baculovirus suspension (5×10^7 plaque-forming units/ml) at a multiplicity of infection of 2.5, containing N-terminally His-tagged, full-length human DEF6, cloned into pFastBac HTB (Invitrogen, Carlsbad, CA). Cultures were grown in Insect Xpress Medium for 48 h for optimal expression. Sf9 cells were collected by centrifugation and lysed in 750 mM NaCl, 20 mM MES pH 7.5, 1% (v/v) Nonidet P-40, 50 mM imidazole, and 1 mM phenylmethanesulfonyl fluoride at 4 °C; and disrupted by sonication at 4 °C. The lysate was cleared by centrifugation at 14,000 $\times$ *g* for 12 min at 4 °C, and the supernatant was incubated with Ni-chelated Sepharose (GE Healthcare). His-tagged DEF6 was eluted from the beads by using 500 mM imidazole at pH 7.5.

ITK kinase domain encompassing residues 352-end (I13–11G, Signal Chem) together with a GST fusion of active full-length ITK and a His fusion of active full-length LCK were obtained from Invitrogen.

In Vitro Kinase Assay—Reactions were assembled containing 150 mM NaCl, 50 mM Hepes pH 7.5, 8 mM $MgCl_2$, 8 mM $MnCl_2$, 100 μM Na_3VO_4, 1 μM ATP, 5 units of recombinant kinase, ~1 μg of substrate and 6 μCi of γ-[^{32}P] ATP. Reactions were incubated for 15 min at 30 °C before being terminated with SDS sample buffer. Samples were analyzed by SDS-PAGE and dried gels were analyzed for incorporation of radioactivity using a Phosphoimager (Fujifilm, FLA-3000). Images were processed using AIDA software.

Cells Culture and Transfection—COS-7 and Jurkat T cell lines were maintained in DMEM or RPMI 1640 culture medium, respectively, at 37 °C and 5% CO_2. Transient transfection of adherent COS-7 cells was performed using Genejuice (Novagen) and grown for 24–48 h prior to microscopy or harvesting of cells for further analysis. In some cases cells were treated with 1 mM sodium arsenite for 30 min. Jurkat T cells in the logarithmic-growth phase were transfected by square-wave electroporation. Cells were re-suspended in complete growth medium at a 4×10^7 cells/ml, and 300 μl of the cell suspension was mixed with 40–50 μg of plasmid DNA in a 4 mm gap electroporation cuvette before being subjected to a single pulse from a BTX ECM 830 electroporator (Harvard Apparatus Inc.) at 310 V for 10 ms. The cells were transferred to culture dishes and incubated for 48 h prior to harvesting for further analysis.

Jurkat T Cell Activation—Transfected Jurkat T cells were activated using a T cell activation and expansion kit (Miltenyi Biotec). Antibiotin-coated magnetic beads were prepared with biotinylated anti-CD2, anti-CD3, and anti-CD28 antibodies as per the manufacturer's instructions. A magnet was used in all steps to retain beads and bound cells. Cells were incubated with beads at 37 °C and 5% CO_2 for 60 min prior to fixation or treated with 100 μm sodium pervanadate (Sigma Aldrich) for 5 min following incubation with beads prior to fixation.

Immunofluorescence—COS-7 cells were grown on coverslips and 48 h after transfection, washed in PBS and fixed for 10 min in freshly-prepared 4% paraformaldehyde, permeabilized with 0.2% Triton X-100 and visualized. Jurkat cells were fixed and permeabilized with 0.1% Tween 20 and resuspended in Vectashield mounting medium containing DAPI (Vector Laboratories) before being mounted on a poly L lysine coated coverslip. F-actin was stained with rhodamine-phalloidin or FITC-phalloidin (Molecular Probes) according to manufacturer's instructions.

Microscope Image Acquisition—Images were taken using either Leica DMRB fluorescent microscope (40× magnification) or Zeiss AXIO Imager.M2 (63× magnification) and acquired using either OpenLab or Axiovison 4.8 software. Images were assembled and labeled in MS PowerPoint and subsequently converted into tiff files using Photoshop.

Cell Lysis and Immunoprecipitation—Transfected cells were collected, and lysed at 10^6 cells/ml in cold lysis buffer (150 mM NaCl, 50 mM Tris pH7.5, 0.1% Nonidet P-40, and 1 mM phenylmethanesulfonyl fluoride). After 30 min at 4 °C, lysates were centrifuged at 4 °C in a microcentrifuge at 14,000 × *g* for 10 min. Supernatants were used directly for immunoprecipitation with α-GFP or α-ITK. The immunoprecipitated proteins and total cell lysates were resolved by SDS-PAGE, transferred to poly (vinylidene difluoride) membranes, immunoblotted using standard procedures. In some cases lysates were prepared as described above and a GST-substrate fusion protein was added before immunoprecipitation.

Bioinformatics—Amino acid sequence of the DHL domain (312–631) of DEF6 were analyzed using the web-based Dotlet program (24) with the block scoring matrix BLOSUM 62 (25), a sliding window of 15, a score range of −60 to 165 and a gray-scale of 39–41% to detect potential short amino acid repeats. The detection of regions with a propensity to form coiled-coils was identified using the web application Paircoil2 (26).

RESULTS

DEF6 Is a Substrate for the Tec-Family Tyrosine Kinase ITK—Previous work identified DEF6 as a substrate for the Src-family kinase LCK and to be phosphorylated on Tyr^{210} (11) and/or Tyr^{133} and Tyr^{144} (5). Given that LCK activates the Tec-family kinase ITK at the immune synapse (16) and since both $ITK^{-/-}$ and $DEF6^{-/-}$ mice exhibit similar autoimmune phenotypes (7, 8, 15), we asked whether DEF6 was also substrate for ITK. Using an *in vitro* kinase assay we showed that His-tagged, full-length human DEF6 isolated from SF9 cells was indeed phosphorylated by both, LCK and ITK (Fig. 1*A*). To substantiate this initial finding, COS-7 cells, that do not express endogenous ITK or DEF6 at detectable levels, were co-transfected with plasmids expressing GFP-tagged DEF6 as the substrate and either DsRed-tagged wild-type mouse ITK (ITK WT) or kinase-dead (K390R) ITK (ITK KD) (16). Immunoblots, probed with the phosphotyrosine-specific monoclonal antibody pY20, revealed that tyrosine phosphorylation of DEF6 was detected in cells co-transfected with ITK WT but not with ITK KD and treated with phosphatase inhibitor pervanadate (Fig. 1*B*). These data established, for the first time, that DEF6 is a substrate for ITK *in vitro* and *in vivo* and suggest that DEF6 is subject to regulation by both Src- and Tec-family kinases at the immune synapse through T cell receptor-mediated signaling.

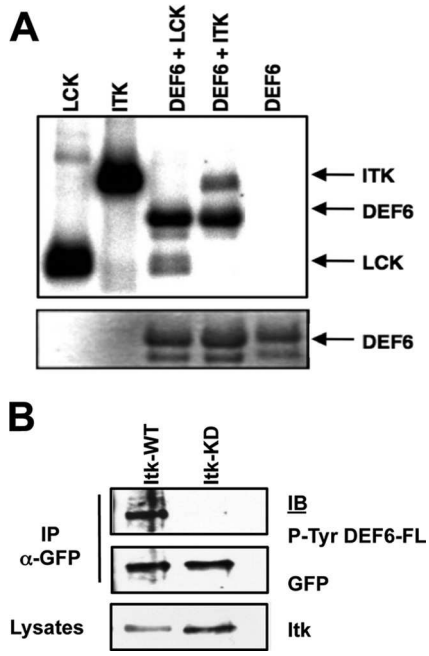

FIGURE 1. **DEF6 is phosphorylated by ITK *in vitro* and *in vivo*.** *A*, *in vitro* kinase assay of His-tagged DEF6 protein isolated from SF9 cells mixed with either active His-tagged LCK or GST-tagged human ITK protein. Auto-phosphorylation of either LCK or ITK alone (as indicated) provided a positive control and recombinant DEF6 protein without any kinase served as a negative control. Coomassie Blue staining confirmed equal loading of His-tagged DEF6 protein (*bottom panel*). *B*, immunoprecipitates (*IPs*) using α-GFP of GFP-tagged DEF6 from COS-7 cells co-transfected with either DsRed-tagged mouse ITK wild-type (ITK WT) or kinase-dead (ITK KD) and treated 48 h after transfection with 100 μM pervanadate for 5 min prior to lysis, were analyzed on SDS-PAGE and subsequently immunoblotted with the antibodies as indicated. Tyrosine phosphorylation of full-length DEF6 was detected using anti-phospho-tyrosine antibody PY20 in the presence of ITK WT but not ITK KD. Western blotting with α-GFP confirmed equal IPs and blotting of the lysates with α-ITK indicated similar amount of ITK WT and ITK KD in each sample.

To determine the tyrosine substrate(s) for ITK phosphorylation we first co-transfected COS-7 cells with GFP-tagged truncation mutants of DEF6 (see Fig. 2*A*) with either ITK WT or ITK KD and analyzed DEF6 phosphorylation using lysates from untreated cells or cells treated with the phosphatase inhibitor pervanadate. As shown in Fig. 2, phosphorylation of the truncation mutants PH-DHL (amino acids 105–631), PH^1 (amino acids 207–330) and PH^2 (amino acids 214–341) was detectable in the pervandate treated samples in the presence of wild-type ITK (Fig. 2*B*). In contrast, ITK KD did not result in any detectable phosphorylation of DEF6 mutant proteins indicating that phosphorylation observed was ITK specific. The DHL domain (355–631) containing a single tyrosine residue (Tyr^{483}) was not phosphorylated by ITK (Fig. 2*B*). These results indicated tyrosines Tyr^{210}, Tyr^{222}, Tyr^{247}, and/or Tyr^{290} of DEF6 as potential targets for ITK phosphorylation. To identify which of these tyrosine residues were phosphorylated by ITK each of the four candidate tyrosine residues was mutated to phenylalanine, either individually or in the case of Tyr^{210} and Tyr^{222} also pair-wise (Fig. 2*A*). Co-transfection of COS-7 cells with plasmid constructs expressing the GFP DEF6 tyrosine mutants and ITK revealed that mutation of either Tyr^{210} or Tyr^{222} to phenylalanine dramatically reduced DEF6 phospho-

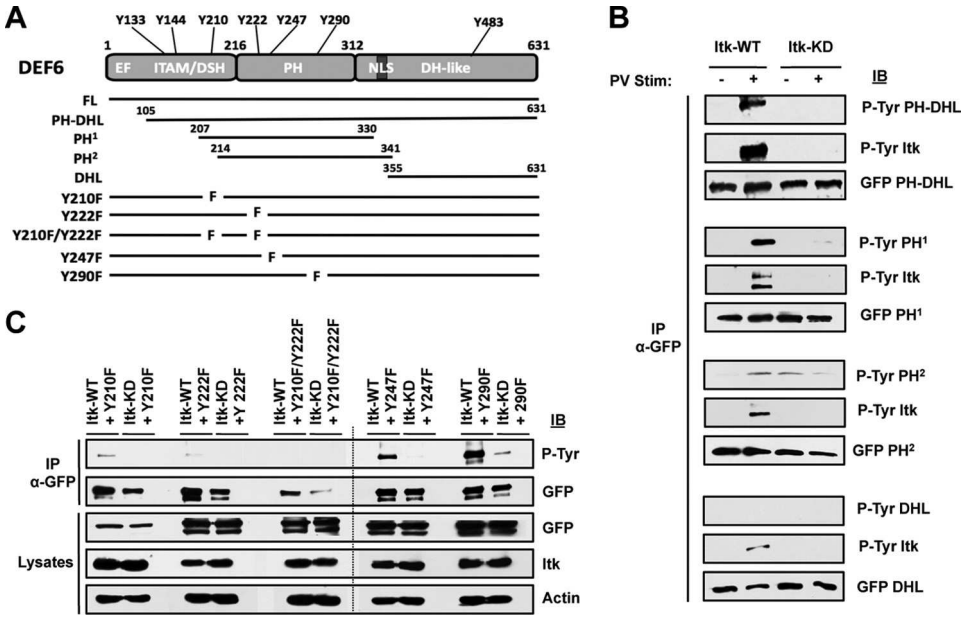

FIGURE 2. **Both tyrosine residues, Tyr^{210} and Tyr^{222}, of DEF6 are phosphorylated by ITK *in vivo*.** *A*, schematic representation of the domain structure of DEF6 indicating the putative Ca^{2+}-binding EF hand, the DEF6-SWAP-70-homology domain (*DSH*) containing a putative immunoreceptor tyrosine-based activation motif (*ITAM*) and the DH-like domain (*DHL*) containing a nuclear localization signal (*NLS*). The position of tyrosines (Y) 133, 144, 210, 222, 247, 290, and 483 are shown. FL and truncation mutants (PH-DHL, PH^1, PH^2, and DHL) as well as tyrosine to phenylalanine (*F*) mutants (*Y210, Y222, Y247, Y290,* and *Y210-Y222*) tagged N-terminally with GFP are schematically depicted as indicated. *B*, GFP-tagged DEF6 truncation mutants (PH-DHL, PH^1, PH^2, DHL) as indicated were co-transfected with either ITK WT or ITK KD tagged with DsRed in COS-7 cells. Cells were either untreated or treated with 100 μM pervanadate (*PV*) for 5 min before lysates were isolated. α-GFP antibodies were used to immunoprecipitate GFP-tagged DEF6 proteins (IP, α-GFP) and after SDS-PAGE, Western blots were performed with the antibodies as indicated (*IB*). To ensure similar amounts of ITK WT and KD protein in each reaction, protein lysates were analyzed by Western blotting shown in Fig. 3*A*. *C*, tyrosine (Y) to phenylalanine (F) DEF6 mutants tagged with GFP were co-transfected with either ITK WT or ITK KD tagged with DsRed in COS-7 cells. Cells were treated with pervanadate as above, and IPs and lysates were analyzed by Western blotting as described in *B*. *Dashed line* indicates that samples were analyzed on two separate gels.

rylation while phosphorylation of the double mutant Y210F-Y222F was undetectable (Fig. 2*C*). In contrast, phosphorylation by ITK of the DEF6 mutants Y249F and Y290F was unaffected (Fig. 2*C*). These data identify two tyrosine residues in close proximity, Tyr^{210} and Tyr^{222}, as substrates for ITK. The three-dimensional structure of DEF6 is unknown; however, Tyr^{210} is predicted to be N-terminal of the PH domain (216–312) and Tyr^{222} to be located within the PH domain.

Interaction between the Kinase Domain of ITK and PH Domain of DEF6 Is Sufficient for Substrate Recognition and Phosphorylation by ITK—Current evidence suggests that substrate recognition by ITK is mediated by interactions at sites that are remote from its catalytic site (27–29). Analysis of the interaction between DEF6 and ITK was initially carried out in COS-7 cells to minimize the possibility of interfering associations with other T cell proteins. In cells co-transfected with GFP-tagged, full-length DEF6 or truncation mutants and wild-type or kinase-dead ITK, it was found that full-length, PH-DHL, and PH^1 formed a stable complex with both active ITK as well as kinase-dead ITK (Fig. 3*A*). As shown above, the GFP-tagged DHL domain on its own was not a substrate for ITK nor did it show any specific interaction with ITK (Fig. 3*A*). To confirm that the interaction between PH domain of DEF6 and ITK also occurs in T cells, GFP-tagged Ph^1, PH^2, DHL, and GFP were co-transfected with either ITK WT or ITK KD in Jurkat cells. As shown in Fig. 3*B* both, Ph^1 and PH^2 but neither DHL nor GFP interacted with ITK. Taken together these results indicate that the PH domain of DEF6 is sufficient to form a stable interaction with ITK, which is independent of its kinase activity. However, we consistently observed stronger signals with active ITK in the presence of pervanadate compared with non-treated cells, a difference not detectable with the kinase-dead mutant (Fig. 3*A*), perhaps suggesting that phosphorylation of DEF6 through ITK results in increased interaction or elevated tyrosine kinase activity in the immune synapse of T cells which may serve to stabilize complexes formed between these proteins to modulate TCR-mediated signaling.

In the case of the two best characterized substrates for ITK; itself, during auto-phosphorylation, and PLCγ1, docking is mediated by an interaction between the kinase domain of ITK and the substrate. To investigate whether interaction of PH domain of DEF6 with ITK was also mediated through the kinase domain of ITK, lysates of COS-7 cells transfected with either full-length or GFP-tagged truncation mutants of DEF6 or GFP alone were incubated with a GST-tagged ITK kinase domain (aa 352–619). Immunoprecipitates using α-GFP antibodies were analyzed by Western blotting using α-GST antibodies. As shown in Fig. 3*C*, the GST-tagged kinase domain of ITK was co-immunoprecipitated with GFP-PH^1 and GFP-PH^2 but not with full-length, PH-DHL, DHL or GFP. Pull down assays of cell lysates from COS-7 transfected with full-length, PH^1 or DHL and incubated with GST alone were performed to demonstrate specificity of this interaction (Fig. 3*C*).

Taken together, these data suggest a model where ITK recognizes DEF6 through an interaction between the kinase domain of ITK and the PH domain of DEF6 that results in the phosphorylation of DEF6 on tyrosine residues 210 and 222 located within and just N-terminal of the PH domain.

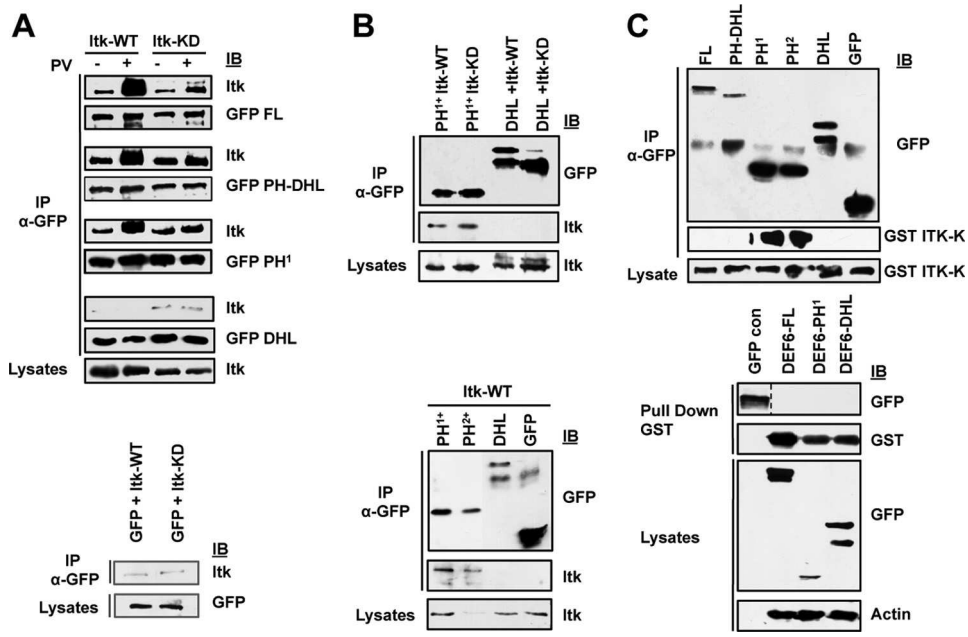

FIGURE 3. **The PH domain of DEF6 interacts with the kinase domain of ITK.** *A*, *upper panel*: GFP-tagged FL DEF6 or truncation mutants (PH-DHL, PH^1, DHL) as indicated were co-transfected with either ITK WT or ITK KD tagged with DsRed in COS-7 cells. Cells were either untreated or treated with 100 μM pervanadate (*PV*) before lysates were isolated. α-GFP antibodies were used to immunoprecipitate GFP-tagged DEF6 proteins (*IP*, α-GFP) and after SDS-PAGE, Western blots were performed with the antibodies as indicated (*IB*). In the case of GFP-DHL, protein lysates were analyzed by Western blotting to ensure similar amounts of ITK WT and KD protein. *Lower panel*: control experiment using lysates from COS-7 cells co-transfected with GFP and either ITK WT or ITK KD indicating minor background signal for ITK co-immunoprecipitated with α-GFP antibodies. *B*, *upper panel*: Jurkat cells were co-transfected with GFP-tagged Ph^1 or DHL truncation mutants with either ITK WT or ITK KD as indicated. Immunoprecipitates using α-GFP antibodies (*IP*, α-GFP) were analyzed by Western blotting (*IB*) to ensure presence of GFP-tagged DEF6 proteins (*GFP*) and test for co-immunoprecipitation of ITK (*ITK*). Total cell lysate was analyzed with α-ITK antibodies to ensure presence of ITK WT and KD proteins (*ITK*). *Lower panel*: Jurkat cells were co-transfected with GFP-tagged Ph^1, PH^2, or DHL truncation mutants as well as GFP alone with ITK WT as indicated. Immunoprecipitates using α-GFP antibodies (*IP*, α-GFP) were analyzed by Western blotting (*IB*) to ensure presence of GFP-tagged DEF6 proteins (*GFP*) and test for co-immunoprecipitation of ITK (*ITK*). Total cell lysate was analyzed with α-ITK antibodies to ensure presence of ITK WT and KD proteins (*ITK*). *C*, *upper panel*: total lysates from COS-7 cells transfected with FL DEF6 or truncation mutants of DEF6 (PH-DHL, PH^1, PH^2, DHL) tagged with GFP and GFP alone was incubated with 80 ng of GST-tagged ITK kinase domain. Immunoprecipitates (*IP*s) using α-GFP antibodies were analyzed by Western blotting (*IB*) to confirm presence of GFP fusion proteins using α-GFP antibodies (*GFP*) and test for co-immunoprecipitation of GST-tagged ITK kinase using α-GST antibodies (*GST ITK-K*). Lysates analyzed using α-GST antibodies (*GST ITK-K*) indicated similar amounts of GST-tagged ITK kinase domain in all extracts. *Lower panel*: COS-7 cell were transfected with the indicated GFP DEF6 plasmids and lysates were incubated with GST (80 ng) as a negative control. GST pull downs were analyzed by immunoblotting with the indicated antibodies (*GST*). α-GFP-positive sample was analyzed alongside the IPs to confirm successful GFP detection.

Formation of DEF6 Cytoplasmic Granules in Response to Cellular Stress—Previous work has demonstrated that phosphorylation of DEF6 at tyrosine residues 133 and 144 by the Src-family kinase LCK is required for targeting DEF6 to the cytoplasmic membrane and subsequent activation NFAT-mediated downstream signaling (5). We investigated whether phosphorylation of DEF6 by ITK, also affected the intracellular targeting of DEF6. COS-7 cells were transfected with GFP-tagged DEF6 or Y210E-Y222E double mutant to mimic the effects of tyrosine phosphorylation by ITK. The intracellular location of the proteins was determined by immunofluorescence (Fig. 4). As previously demonstrated (2) wild-type DEF6 was spread diffusely throughout the cytoplasm demonstrating that overexpression of DEF6 does not result in granule formation *per se* (Fig. 4*A*). In contrast, the phosphomimic Y210E-Y222E protein spontaneously aggregated and formed cytoplasmic granules (Fig. 4*B*). Granule formation was not observed however when phosphomimic mutants with single tyrosine to glutamate changes (Y210E, Y222E, Y247E, or Y290E; supplemental Fig. S1) were expressed as GFP fusion proteins suggesting that granule formation is not due to abnormal folding of phosphomimic mutants *per se*. Rather, these findings suggest that the introduction of negative charges at residues 210 and 222 through tyrosine phosphorylation of DEF6 by ITK results in a conformational change that unmasks regions that promote aggregation. The granules formed by the Y210E-Y222E mutant were morphologically similar to stress granules (SG) and processing bodies (P-bodies), which are discrete ribonucleoprotein granules that regulate gene expression by delaying the translation of specific transcripts and are recognized to play a role in regulating the immune response (30, 31). We therefore asked whether treatment with reagents that arrest mRNA translation would result in the formation of wild-type DEF6 granules. Sodium arsenite and puromycin are frequently used to generate stress granules and P-bodies as they cause sudden translational arrest and accumulation of stalled translation initiation complexes (32, 33). Indeed, treatment of COS-7 cells expressing GFP-tagged DEF6 with sodium arsenite or puromycin resulted in the formation of DEF6 granules (Fig. 4, *C* and *E*), similar in appearance to those observed for the Y210E-Y222E mutant (Fig. 4*B*) but not observed upon treatment of GFP transfected cells (Fig. 4, *D* and *F*). It seems therefore that DEF6 can adopt at least two structural conformations in cells; one maintains it as a soluble protein and the other results in self-aggregation and the formation of cytoplasmic granules. It is likely that phosphorylation at tyrosines 210 and 222 by the Tec kinase ITK consti-

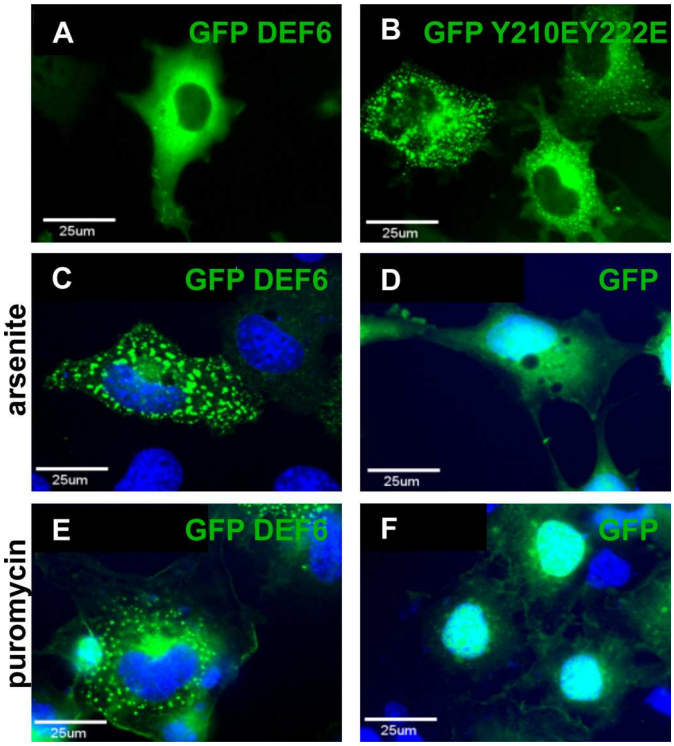

FIGURE 4. **Formation of cytoplasmic granules by the phosphomimic Y221E-Y222E mutant or wild-type DEF6 protein in response to cellular stress in COS-7 cells.** COS-7 cells transfected with wild-type (*WT*) DEF6 tagged with GFP exhibit a homogeneous cytoplasmic localization of DEF6 (*A*). In contrast, the Y210E-Y222E double mutant, mimicking ITK phosphorylation of DEF6, tagged to GFP aggregates, and forms cytoplasmic granules (*B*). Sodium arsenite treatment (1 mM, 30 min) of COS-7 cells transfected with wild-type (*WT*) DEF6 tagged with GFP results in granule formation (*C*) not observed in control cells transfected with GFP (*D*). Puromycin treatment (0.25 mg/ml, 2 h) of COS-7 cells transfected with wild-type (WT) DEF6 tagged with GFP results in granule formation (*E*) not observed in control cells transfected with GFP (*F*). Nuclei are stained with DAPI (*blue*). Images were taken with 40× magnification. Scale bars: 25 μm.

tutes one of the modifications of DEF6 that results in a conformational change causing aggregation but because ITK is not expressed in COS-7 cells, it is also clear that a similar switch in the conformation of DEF6 can be induced by the activation of signaling events that take place in response to cell stress or inhibition of translation.

Altered Localization and Function of Wild-type and Y210E-Y222E DEF6 Mutant upon T Cell Receptor-mediated Signaling—It was previously shown that TCR-mediated signaling resulted in phosphorylation of DEF6 by LCK and subsequent recruitment of DEF6 to the immunological synapse (11). To establish whether phosphorylation of DEF6 had any effect on the localization of DEF6 at the IS, we transfected Jurkat cells with wild-type or the phosphomimic Y210E-Y222E mutant DEF6 and stimulated the cells with anti-CD2, CD3 and anti-CD28 coated 3.5 μm magnetic beads. As shown in Fig. 5, wild-type GFP DEF6 protein was recruited to the IS as expected (Fig. 5*B*). In contrast, the Y210E-Y222E mutant DEF6 protein formed aggregates but the localization of the phosphomimic mutant was clearly distinct from the GFP-tagged wild-type DEF6 protein (Fig. 5*C*). Similar results where obtained when 10 μm polystyrene beads coated with anti CD3 (Okt3) and anti CD28 antibodies were used to induce IS formation in transfected Jurkat cells (supplemental Fig. S2) demonstrating that localization of wild-type and Y210E-Y222E DEF6 mutant proteins in Jurkat cells is independent of the size of the beads used to induce synapse formation. To further dissect the role of phosphorylation on DEF6 function we treated the transfected Jurkat cells with pervanadate to inhibit phosphatases and prevent dephosphorylation of DEF6. Such treatment that had no effect on the localization of GFP (Fig. 5*D*), but caused a dramatic change in the localization of the GFP-tagged wild-type DEF6 protein. It was no longer concentrated in the IS but rather distributed throughout the cytoplasm and exhibited some aggregate formation (Fig. 5*E*). These data suggest that prolonged and uncontrolled phosphorylation of DEF6 results in a redistribution of DEF6 and apparent GEF activity throughout the cytoplasm to the extent that Jurkat cells exhibited filopodia formation, highlighted by the staining with phalloidin (Fig. 5*E*, *boxed enlargement in middle panel*). In clear contrast, pervanadate treatment of Jurkat cells transfected with the Y210E-Y222E mutant did not show any redistribution of the mutant protein that still formed aggregates (Fig. 5*F*).

Together these results suggest that phosphorylation of DEF6 by ITK causes cellular redistribution and aggregate formation and they are consistent with the recent observation that DEF6 localization in T cells is dependent upon ITK function (18).

DEF6 Cytoplasmic Granules Co-localize with DCP1, a Marker for P-bodies—Proteins that contain self-aggregation domains such as the RNA-binding proteins TIA-R, TIA-1, and G3BP are a hallmark of SGs and P-bodies (34) and we therefore tested whether DEF6 granules were associated with either SGs or P-bodies. Co-transfection of COS-7 cells using GFP DEF6 constructs in combination with DsRed-tagged mRNA decapping enzyme 1 (DCP1), a marker for P-bodies, revealed that wild-type GFP DEF6, similar to GFP alone, did not significantly overlap with DCP1 (Fig. 6, *A* and *B*). In contrast, arsenite treatment resulted in cytoplasmic granule formation of GFP DEF6 that clearly co-localized with DsRed DCP1 (Fig. 6*E*) whereas arsenite treatment did not affect localization of the GFP protein (Fig. 6*D*). The spontaneously self-aggregating Y210E-Y222E DEF6 mutant however, mostly co-localized with DsRed DCP1 independently of arsenite treatment (Fig. 6, *C* and *F*, see also *boxed enlargement*) suggesting that post-translational modification through phosphorylation of DEF6 is sufficient to cause self-aggregation and P-body localization. The presence of partly overlapping granules and co-localizing granules suggests a dynamic interaction between DEF6 granules and P-bodies.

To test whether altered localization and function of the Y210E-Y222E DEF6 mutant in activated Jurkat cells was associated with P-bodies we analyzed Jurkat cells co-transfected with wild-type or mutant GFP DEF6 and DsRed DCP1 and stimulated the cells with anti-CD2, CD3 and CD28 antibodies conjugated to magnetic beads. DsRed DCP1 on its own formed cytoplasmic granules that were independent from TCR-mediated activation and IS formation as shown in Fig. 7*A*. The continual presence of P-bodies is characteristic of a number of cell lines (34). Wild-type GFP DEF6 co-transfected with DsRed DCP1 into Jurkat cells was recruited to the IS and did not form aggregates that co-localized with DsRed DCP1 (Fig. 7*B*). In contrast, aggregates formed by the Y210E-Y222E DEF6 mutant co-

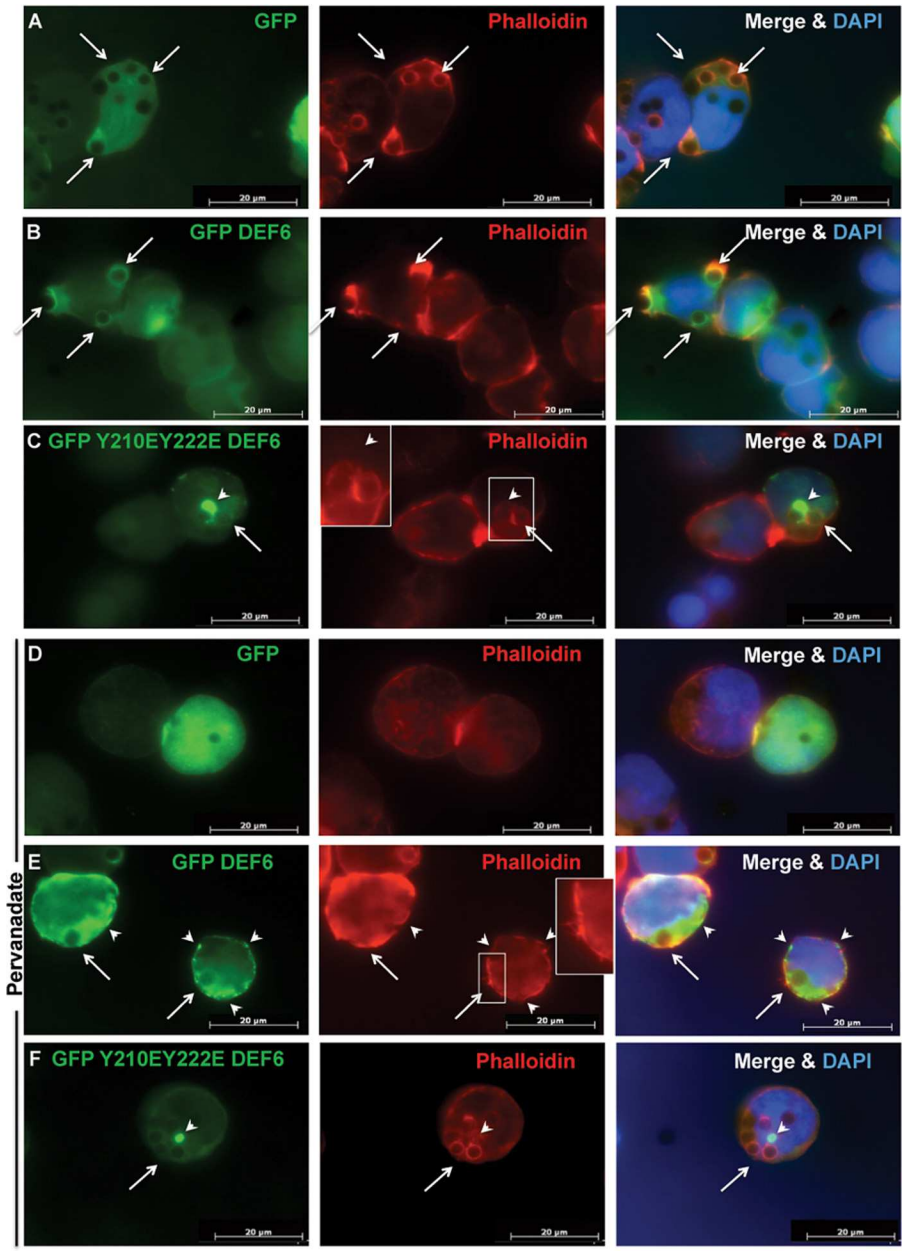

FIGURE 5. **Formation of cytoplasmic granules by the phosphomimic Y221E-Y222E mutant or wild-type DEF6 protein after pervanadate treatment in Jurkat cells.** Jurkat cells transfected with GFP (*A*, *D*), GFP-tagged DEF6 (*B*, *E*), or GFP-tagged phosphomimic Y221E-Y222E mutant (*C*, *F*) were incubated with magnetic beads conjugated with anti-CD2, anti-CD3 and anti-CD28 antibodies and either left untreated (*A–C*) or treated with pervanadate (*D–F*) and subsequently stained with rhodamin-phalloidin and DAPI. Images were taken with 63× magnification and pseudo-colored using Axiovision software. GFP (*green*), phalloidin (*red*), and the merged images including DAPI (*blue*) are shown. *Arrows* indicate position of magnetic beads; *arrowheads* indicate cytoplasmic granules. Scale bars: 20 μm.

localized with DsRed DCP1 (Fig. 7*C*). Pervanadate treatment resulted in re-distribution the GFP DEF6 wild-type protein as shown before and some aggregates formed co-localized with DsRed DCP1 (Fig. 7*E*) whereas aggregates formed by the Y210E-Y222E DEF6 mutant completely overlapped with DsRed DCP1 (Fig. 7*F*).

The DHL Domain of DEF6 Is Glutamine-rich and Contains Heptad Repeats that Are Likely to Adopt a Coiled-coil Formation Mediating Self-aggregation—Having established that DEF6 has the capacity to form cytoplasmic granules we analyzed its primary sequence for the presence of amino acids that could explain its self-aggregation properties. A prominent feature of the sequence of DEF6 is that it is inordinately rich in the amino acid glutamine (10%), a characteristic of many amyloid-forming proteins, and glutamic acid (12.2%). Significantly, both amino acids are concentrated within the DHL-domain of DEF6 (Q, 15.4%; E, 17.2%). In amyloid-forming proteins, glutamine is generally believed to promote protein aggregation through the formation of β-sheets that could provide the molecular basis for DEF6 granule formation. However, the abundance of polar and charged residues that destabilize or break β-sheets (35) in the same region makes this unlikely. We therefore looked for an alternative mechanism to explain granule formation. Based on recent findings that coiled-coil-forming regions in Q/N-rich

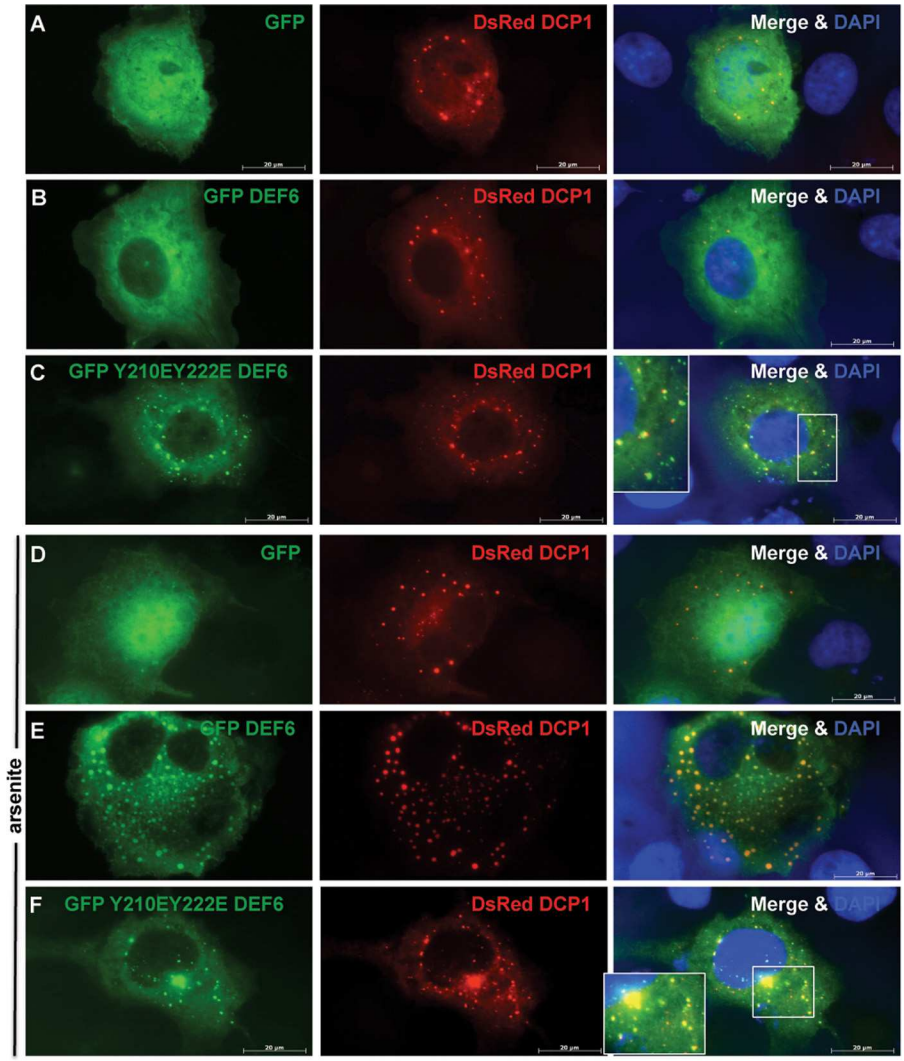

FIGURE 6. **DEF6 cytoplasmic granules co-localize with the P-body protein DCP1 in COS-7 cells.** COS-7 cell co-transfected with DsRed DCP1 and either, GFP (*A*, *C*), GFP-tagged DEF6 (*B*, *E*) or GFP-tagged phosphomimic Y221E-Y222E mutant (*C*, *F*) were left untreated (*A–C*) or treated with sodium arsenite (*D–F*) and subsequently stained with DAPI. Images were taken with 63× magnification and pseudo-colored using Axiovision software. GFP (*green*), DsRed DCP1 (*red*), and the merged images including DAPI (*blue*) are shown. Scale bars: 20 μm.

prions and poly Q proteins promote aggregation (22), we considered this mechanism for DEF6 aggregation. Using Paircoil2, an algorithm that detects coiled-coil-forming heptad repeats in primary sequences (26), a region of 220 amino acids (Arg^{330}-Leu^{550}) within the DHL-domain was identified that is predicted to have a high probability of forming coiled-coils (<0.025) (Fig. 8*A*). The occurrence of a hydrophobic amino acid or glutamine, an ambivalent hydrophobe, at the "a" and "d" positions in an alpha helix is essential for them to appear on the same side of the helix and provide the hydrophobic interactions necessary for the formation of a coiled-coil. The hydrophobic and glutamine residues between Arg^{330} and Leu^{550} frequently occupy the "a" and "d" positions in 28 heptad repeats (Fig. 8*B*). The prediction for the propensity for DEF6 to form coiled-coils is very similar to that of tropomyosin; the archetypal coiled-coil forming protein (36) (Fig. 8*A*) and appears to be a feature that, in its role as a GEF, is unique to DEF6. Other Rho GEFs Dbs and Vav1 are neither predicted to contain regions of coiled-coil by the program Paircoil2, nor are coiled-coils observed in their structures derived from x-ray crystallographic studies (37, 38) and (Fig. 8*A*). Analysis of the sequence of the DHL domain (amino acids 312–631) using a diagonal plot to identify repeats of similar amino acid sequences (24) revealed that, based on sequence complexity, the DHL domain consists of two distinct regions (Fig. 8*C*). Approximately, the N-terminal two-thirds of DEF6 (Arg^{312}-Arg^{521}) consists of glutamine- and glutamate-enriched stretches of amino acids that are repeated through this region. In contrast, the C-terminal third of the DHL domain is more complex as no repeat sequences are found in this region, which suggests a different function. The abundance of glutamines in the N-terminal portion of the DHL domain (40/209 or 19%) suggested that this region is involved in granule formation in response to phosphorylation of DEF6 by ITK or cellular stress. To test this, GFP fusion proteins of the N-terminal region of the DHL domain (311–501) and C-terminal region (476–591) were expressed in COS-7 cells. As anticipated the glutamine-rich N-terminal region of the DHL domain formed cytoplasmic granules while the C-terminal region remained diffuse in the cytoplasm (Fig. 8*C*). These data fully support the predictions that the glutamine-rich N-terminal region of the DHL domain

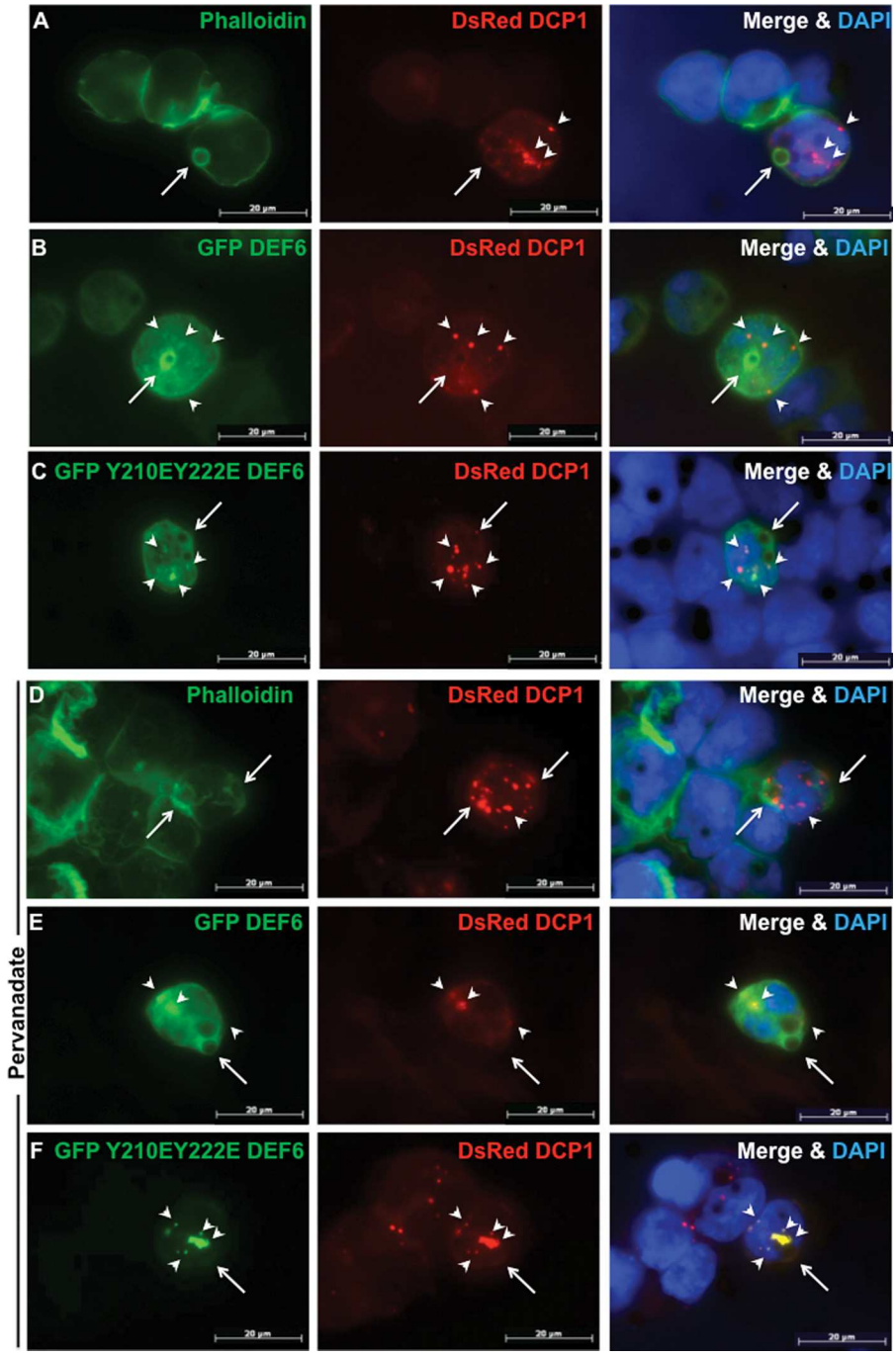

FIGURE 7. **DEF6 cytoplasmic granules co-localize with the P-body protein DCP1 in Jurkat cells.** Jurkat cells transfected with DsRed DCP1 alone (*A*, *D*) or co-transfected with GFP-tagged DEF6 (*B*, *E*) or GFP-tagged phosphomimic Y221E-Y222E mutant (*C*, *F*) were incubated with magnetic beads conjugated with anti-CD2, anti-CD3, and anti-CD28 antibodies and either left untreated (*A–C*) or treated with pervanadate (*D–F*), and subsequently stained with FITC-phalloidin (*A*, *D*) and DAPI (*A–F*). Images were taken with 63× magnification and pseudo-colored using Axiovision software. GFP (*green*), phalloidin (*green*), and the merged images including DAPI (*blue*) are shown. *Arrows* indicate position of magnetic beads; *arrowheads* indicate cytoplasmic granules. Scale bars: 20 μm.

of DEF6 is responsible for self-aggregation, cytoplasmic granule formation and P-body localization

Cumulatively, our data suggest that DEF6 is able to switch between a soluble and granule-forming conformation that is likely to be triggered through phosphorylation by ITK or similar post-translational modifications induced by conditions of cell stress. Mechanistically, aggregation is probably mediated by coiled-coil forming, heptad repeats that are enriched in the glutamine-rich DHL domain. This unusual property of DEF6 may be reflected in the orientation of the PH and DHL domains that is atypical of other Rho-family GEFs and found only in SWAP-70, the closest relative of DEF6.

DISCUSSION

DEF6 is a novel Rho-family GEF that is predominantly expressed in T cells. Upon T cell receptor-mediated signaling, DEF6 is recruited to the immunological synapse following phosphorylation by LCK. Initially, tyrosine 210 of DEF6 was

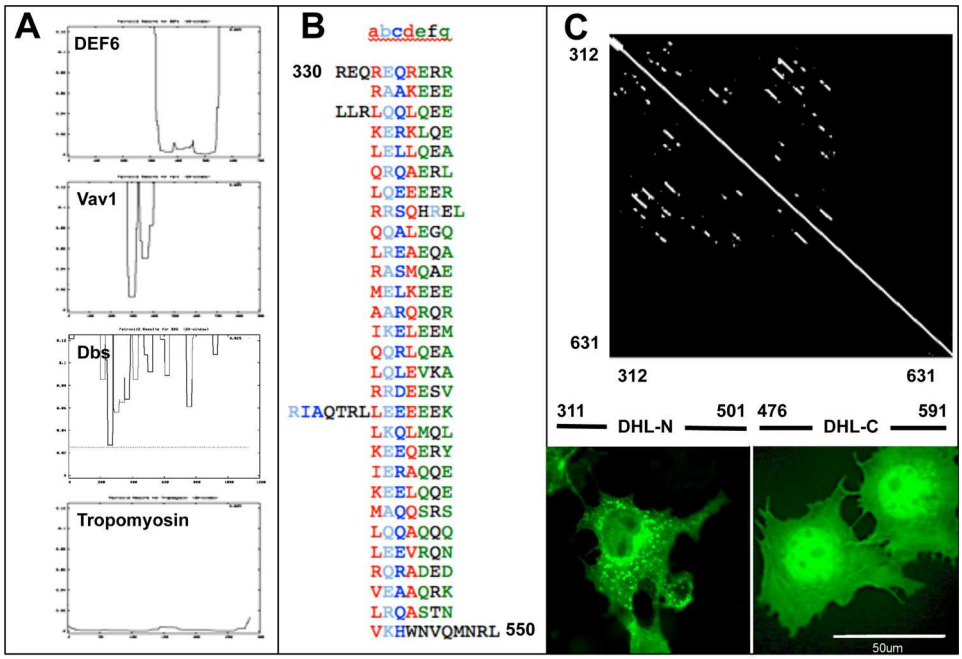

FIGURE 8. **Protein aggregation and granule formation of DEF6 is mediated through a coiled-coil region in the N-terminal part of the DHL domain.** *A*, prediction of the probability of the proteins DEF6, Vav1, Dbs, and tropomyosin as indicated to form a coiled-coil using the program Paircoil2 with an amino acid window length of 28. Residues with a value below 0.025 (*dotted line*) are predicted to have a high probability to exist in a coiled-coil. *B*, occurrence of glutamines (Q) or hydrophobic amino acids at the "*a*" and "*d*" position of the heptad repeats (*a–g*) of the predicted coiled-coil region between amino acids 330 and 550 of DEF6. Glutamines and hydrophobic residues at these positions are essential for coiled-coil formation in well-characterized, coiled-coil forming proteins like Tropomyosin. *C*, *upper panel*: diagonal plot of amino acids 312–631 of DEF6 plotted against the same region illustrating the repeats of similar sequences between Arg^{312} and Arg^{521}, which contrasts with the remaining C-terminal sequence. The plot was generated with the program Dotlet using the BLOSUM 62 scoring matrix and a sliding window of 15. The score matrix was −60 to −165 with a greyscale of 39–41%. *Lower panel*: N-terminal part of the DHL domain (amino acids 311–501) is sufficient to form cytoplasmic granules when expressed as a GFP fusion protein in COS-7 cells. In contrast, the C-terminal part of the DHL domain (amino acids 476–591) when expressed as a GFP fusion protein in COS-7 cells is localized through out the cytoplasm and nuclei. Localization of the fusion protein in the nucleus is likely a result of passive diffusion of low-molecular weight proteins through the nuclear membrane. Images were taken with 40× magnification. Scale bar: 50 μm.

identified as the site of tyrosine phosphorylation by LCK (11), but subsequent work identified tyrosines 133 and 144 that are proposed to constitute an ITAM-like sequence as substrates for LCK (5). Analysis of DEF6 knock-out mice demonstrated that DEF6 phosphorylation and translocation to the immunological synapse was required for Ca^{2+} signaling and activation of the transcription factor NFAT, regulating Th1 and Th2 inflammatory responses (5, 6). Depending on the genetic background, DEF6-deficient mice exhibited spontaneous development of systemic autoimmunity (39) mediated through uncontrolled activity of IRF-4 transcriptional regulation and overproduction of IL-17 and IL-21 (8) or were resistant to Th1/Th17-mediated Experimental Autoimmune Encephalomyelitis due to deficient differentiation into Th17 cells (7); see also (40). These results established DEF6 as an essential component of the T cell receptor-mediated signal transduction pathway, regulating not only actin cytoskeleton reorganization but also many crucial effector functions similar to the well characterized Rho-family GEF Vav1 (41). However, some aspects of DEF6-deficiency, such as effects on Ca^{2+} signaling, activation of the transcription factor NFAT and IL-17A expression have been described in ITK-deficient mice (15, 42, 43) which prompted us to test whether DEF6 was a substrate for ITK, a member of the Tec-family of tyrosine kinases. Most recently an important functional link between ITK and DEF6 has been established at the immune synapse where ITK has been identified as necessary for the localization of DEF6 to this region and for actin remodeling in this signal-transducing structure (18). Here we show that DEF6 is a direct substrate for ITK and is phosphorylated at tyrosines 210 and 222. This is in clear contrast to the GEF Vav1 that is not a substrate for ITK (44, 45); although a kinase-independent adaptor function of ITK is necessary for TCR-induced regulation of Vav1 and the actin cytoskeleton (46). Significantly, full-length DEF6, or truncated versions of DEF6 that contained the PH domain, were necessary for mediating the interaction with ITK, associated with both active and kinase-dead ITK. Furthermore, interaction of the PH domain of DEF6 with ITK is mediated through the kinase domain of ITK, which has also been found to be the case for the best characterized substrates of ITK (28, 47). Since LCK is both responsible for ITK activation by phosphorylating it at tyrosine 511 (16) and targeting DEF6 to the cell membrane by phosphorylation of tyrosines 133 and 144 (5) this places LCK as the key upstream regulator of DEF6 phosphorylation at tyrosine residues 210 and 222 by ITK. Consequently, phosphorylation at tyrosine 210 of DEF6 by ITK is ultimately dependent on LCK activity. Our findings might go some way in explaining why phosphorylation of tyrosine 210 was originally attributed to LCK (11).

In experiments to determine whether phosphorylation of DEF6 at tyrosines 210 and 222 by ITK affected its intracellular location and therefore potential function, we were surprised to find that the phosphomimic DEF6 Y210E-Y222E mutant protein, accumulated in cytoplasmic granules. The formation of these granules was not due to nonspecific aggregation, since

wild-type DEF6 distributed mainly diffusely throughout the cytoplasm, strongly suggesting that the presence of negative charges at residues 210 and 222, and therefore by implication phosphorylation by ITK, triggers a change in the conformation of DEF6 that results in aggregation. Cytoplasmic granule formation was also observed in COS-7 cells transfected with GFP DEF6 when treated with arsenite or puromycin; two agents that induce cell stress and formation of granules involved in post-transcriptional regulation such as P-bodies and stress granules (21). This indicates that the switch in conformation of DEF6 is also regulated by mechanisms other than by ITK phosphorylation that are associated with changes in translational regulation. An analysis of the primary sequence of DEF6 immediately identified an abundance of glutamine (Q), concentrated in the DHL domain not found in any other Rho GEF. Glutamine-rich sequences are found in many proteins prone to aggregation through the formation of β-sheets (48, 49) and suggests that DEF6 would have a propensity to aggregate. Paradoxically, the DHL domain is also very rich in glutamate and other charged residues which destabilise β-sheet formation (35), which forced us to consider another explanation for aggregation. Recently, a role for coiled-coils in the formation of aggregates by glutamine-rich proteins has been elucidated (22). Coiled-coils are formed between proteins that contain repeats of seven amino acids (a-b-c-d-e-f-g) in which hydrophobic residues often occupy positions a/d to form a hydrophobic layer between the coiling helices; one of the best examples being the protein tropomyocin (36). Consequently, we identified putative coiled-coil-forming heptads within the DHL domain of DEF6 that we propose provide the structural basis of DEF6 aggregation. The mechanism whereby DEF6 is able to switch between a soluble and aggregate forming protein remains to be explored. However, as the presence of a trigger sequence within the coiled-coil region has been found to be essential to nucleate and promote the formation of in-register, productive chain associations (51), it is plausible that a trigger sequence may exist within the DHL domain of DEF6 that is unmasked by ITK phosphorylation or cell-stress signals. Compatible with this, it might be significant that GFP-DHL fusion proteins always appear as two species with different apparent sizes on immunoblots (see Fig. 3, *B* and *C*), which is consistent with the formation of an SDS-resistant aggregate once the DHL domain has been freed of constraints on its conformation that might be imposed by N-terminal sequences. A requirement for DEF6 to change conformation to fulfill its role in T cells may explain why evolutionary selection pressure has maintained the N- to C-terminal PH-DHL domain organization that is atypical of Rho-family GEFs.

Even if the extent of DEF6 granule formation we observed in transfection experiments is exaggerated, non-the-less, our data demonstrate that DEF6 has the potential to undergo a switch between a soluble and granule-forming protein. The co-localization of DEF6 granules with P-bodies; cytoplasmic granules involved in mRNA degradation, strongly suggests a role for DEF6 in the regulation of mRNA translation. Our observations that the association between DEF6 granules and P-bodies change depending on phosphorylation or perturbation of mRNA translation suggest that the interaction between these granules are dynamic and may be regulated through interaction between glutamine-rich sequences found in DEF6 and in P-body and Stress granule proteins (52, 53) or may require the recruitment of other molecules to modulate their interaction. The importance of regulation at the mRNA level in the immune response is now becoming increasingly evident (30, 50). We propose that DEF6 not only regulates signal transduction from the immune synapse through its activity as a Rho GEF but as indicated by its structural and biochemical properties, DEF6 may also have some role in regulating mRNA translation in response to TCR-mediated signaling.

Acknowledgments—We thank Maria Isabel Haig, Louis Brailsford, and Eleanor Mollett for technical help, Dr. T. Samson (University of North Carolina), Drs. S. Wheatley, T. Sharp (University of Nottingham), Y. Shav-Tal (Bar Ilan University, Israel), and P. Schwartzberg (NIH, Bethesda, MD) for providing helpful reagents, to Drs. Y-J. Yeh and I. Kerr (University of Nottingham) for help with the baculoviral system and B. McConnochie, A. Diamond, M. Rennie, R. Tsikandelova, and J. Zheng for help with COS-7 cell transfections.

REFERENCES

1. Hotfilder, M., Baxendale, S., Cross, M. A., and Sablitzky, F. (1999) Def-2, -3, -6, and -8, novel mouse genes differentially expressed in the haemopoietic system. *Br. J. Haematol* **106,** 335–344
2. Mavrakis, K. J., McKinlay, K. J., Jones, P., and Sablitzky, F. (2004) DEF6, a novel PH-DH-like domain protein, is an upstream activator of the Rho GTPases Rac1, Cdc42, and RhoA. *Exp. Cell Res.* **294,** 335–344
3. Tanaka, Y., Bi, K., Kitamura, R., Hong, S., Altman, Y., Matsumoto, A., Tabata, H., Lebedeva, S., Bushway, P. J., and Altman, A. (2003) SWAP-70-like adapter of T cells, an adapter protein that regulates early TCR-initiated signaling in Th2 lineage cells. *Immunity* **18,** 403–414
4. Gupta, S., Lee, A., Hu, C., Fanzo, J., Goldberg, I., Cattoretti, G., and Pernis, A. B. (2003) Molecular cloning of IBP, a SWAP-70 homologous GEF, which is highly expressed in the immune system. *Hum. Immunol.* **64,** 389–401
5. Bécart, S., Balancio, A. J., Charvet, C., Feau, S., Sedwick, C. E., and Altman, A. (2008) Tyrosine-phosphorylation-dependent translocation of the SLAT protein to the immunological synapse is required for NFAT transcription factor activation. *Immunity* **29,** 704–719
6. Bécart, S., Charvet, C., Canonigo Balancio, A. J., De Trez, C., Tanaka, Y., Duan, W., Ware, C., Croft, M., and Altman, A. (2007) SLAT regulates Th1 and Th2 inflammatory responses by controlling Ca2+/NFAT signaling. *J. Clin. Invest.* **117,** 2164–2175
7. Canonigo-Balancio, A. J., Fos, C., Prod'homme, T., Bécart, S., and Altman, A. (2009) SLAT/Def6 plays a critical role in the development of Th17 cell-mediated experimental autoimmune encephalomyelitis. *J. Immunol.* **183,** 7259–7267
8. Chen, Q., Yang, W., Gupta, S., Biswas, P., Smith, P., Bhagat, G., and Pernis, A. B. (2008) IRF-4-binding protein inhibits interleukin-17 and interleukin-21 production by controlling the activity of IRF-4 transcription factor. *Immunity.* **29,** 899–911
9. Tybulewicz, V. L. (2005) Vav-family proteins in T-cell signalling. *Curr. Opin. Immunol.* **17,** 267–274
10. Borggrefe, T., Wabl, M., Akhmedov, A. T., and Jessberger, R. (1998) A B-cell-specific DNA recombination complex. *J. Biol. Chem.* **273,** 17025–17035
11. Gupta, S., Fanzo, J. C., Hu, C., Cox, D., Jang, S. Y., Lee, A. E., Greenberg, S., and Pernis, A. B. (2003) T cell receptor engagement leads to the recruitment of IBP, a novel guanine nucleotide exchange factor, to the immunological synapse. *J. Biol. Chem.* **278,** 43541–43549
12. Andreotti, A. H., Schwartzberg, P. L., Joseph, R. E., and Berg, L. J. (2010) T-cell signaling regulated by the Tec family kinase, Itk. *Cold Spring Harb. Perspect. Biol.* **2,** a002287
13. Salmond, R. J., Filby, A., Qureshi, I., Caserta, S., and Zamoyska, R. (2009)

T-cell receptor proximal signaling via the Src-family kinases, Lck and Fyn, influences T-cell activation, differentiation, and tolerance. *Immunol. Rev.* **228,** 9–22
14. Wang, H., Kadlecek, T. A., Au-Yeung, B. B., Goodfellow, H. E., Hsu, L. Y., Freedman, T. S., and Weiss, A. (2010) ZAP-70: an essential kinase in T-cell signaling. *Cold Spring Harb. Perspect Biol.* **2,** a002279
15. Gomez-Rodriguez, J., Sahu, N., Handon, R., Davidson, T. S., Anderson, S. M., Kirby, M. R., August, A., and Schwartzberg, P. L. (2009) Differential expression of interleukin-17A and -17F is coupled to T cell receptor signaling via inducible T cell kinase. *Immunity* **31,** 587–597
16. Heyeck, S. D., Wilcox, H. M., Bunnell, S. C., and Berg, L. J. (1997) Lck phosphorylates the activation loop tyrosine of the Itk kinase domain and activates Itk kinase activity. *J. Biol. Chem.* **272,** 25401–25408
17. Wilcox, H. M., and Berg, L. J. (2003) Itk phosphorylation sites are required for functional activity in primary T cells. *J. Biol. Chem.* **278,** 37112–37121
18. Singleton, K. L., Gosh, M., Dandekar, R. D., Au-Yeung, B. B., Ksionda, O., Tybulewicz, V. L., Altman, A., Fowell, D. J., and Wülfing, C. (2011) Itk controls the spatiotemporal organization of T cell activation. *Sci. Signal* **4,** ra66
19. Anderson, P., and Kedersha, N. (2009) RNA granules: post-transcriptional and epigenetic modulators of gene expression. *Nat. Reviews* **10,** 430–436
20. Buchan, J. R., and Parker, R. (2009) Eukaryotic stress granules: the ins and outs of translation. *Mol. Cell* **36,** 932–941
21. Kedersha, N., and Anderson, P. (2007) Mammalian stress granules and processing bodies. *Methods Enzymol.* **431,** 61–81
22. Fiumara, F., Fioriti, L., Kandel, E. R., and Hendrickson, W. A. (2010) Essential role of coiled coils for aggregation and activity of Q/N-rich prions and PolyQ proteins. *Cell* **143,** 1121–1135
23. Samson, T., Will, C., Knoblauch, A., Sharek, L., von der Mark, K., Burridge, K., and Wixler, V. (2007) Def-6, a guanine nucleotide exchange factor for Rac1, interacts with the skeletal muscle integrin chain α7A and influences myoblast differentiation. *J. Biol. Chem.* **282,** 15730–15742
24. Junier, T., and Pagni, M. (2000) Dotlet: diagonal plots in a web browser. *Bioinformatics* **16,** 178–179
25. Henikoff, S., and Henikoff, J. G. (1992) Amino acid substitution matrices from protein blocks. *Proc. Natl. Acad. Sci. U.S.A.* **89,** 10915–10919
26. McDonnell, A. V., Jiang, T., Keating, A. E., and Berger, B. (2006) Paircoil2: improved prediction of coiled coils from sequence. *Bioinformatics* **22,** 356–358
27. Joseph, R. E., Min, L., Xu, R., Musselman, E. D., and Andreotti, A. H. (2007) A remote substrate docking mechanism for the tec family tyrosine kinases. *Biochemistry* **46,** 5595–5603
28. Min, L., Joseph, R. E., Fulton, D. B., and Andreotti, A. H. (2009) Itk tyrosine kinase substrate docking is mediated by a nonclassical SH2 domain surface of PLCγ1. *Proc. Natl. Acad. Sci. U.S.A.* **106,** 21143–21148
29. Joseph, R. E., Severin, A., Min, L., Fulton, D. B., and Andreotti, A. H. (2009) SH2-dependent autophosphorylation within the Tec family kinase Itk. *J. Mol. Biol.* **391,** 164–177
30. Anderson, P. (2010) Post-transcriptional regulons coordinate the initiation and resolution of inflammation. *Nat. Rev. Immunol.* **10,** 24–35
31. Anderson, P. (2008) Post-transcriptional control of cytokine production. *Nat. Immunol.* **9,** 353–359
32. Kedersha, N., Cho, M. R., Li, W., Yacono, P. W., Chen, S., Gilks, N., Golan, D. E., and Anderson, P. (2000) Dynamic shuttling of TIA-1 accompanies the recruitment of mRNA to mammalian stress granules. *J. Cell Biol.* **151,** 1257–1268
33. Kedersha, N. L., Gupta, M., Li, W., Miller, I., and Anderson, P. (1999) RNA-binding proteins TIA-1 and TIAR link the phosphorylation of eIF-2α to the assembly of mammalian stress granules. *J. Cell Biol.* **147,** 1431–1442
34. Kedersha, N., Tisdale, S., Hickman, T., and Anderson, P. (2008) Real-time and quantitative imaging of mammalian stress granules and processing bodies. *Methods Enzymol.* **448,** 521–552
35. Colloc'h, N., and Cohen, F. E. (1991) Beta-breakers: an aperiodic secondary structure. *J. Mol. Biol.* **221,** 603–613
36. Hitchcock-DeGregori, S. E. (2008) Tropomyosin: function follows structure. *Adv. Exp. Med. Biol.* **644,** 60–72
37. Rossman, K. L., Worthylake, D. K., Snyder, J. T., Siderovski, D. P., Campbell, S. L., and Sondek, J. (2002) A crystallographic view of interactions between Dbs and Cdc42: PH domain-assisted guanine nucleotide exchange. *EMBO J.* **21,** 1315–1326
38. Yu, B., Martins, I. R., Li, P., Amarasinghe, G. K., Umetani, J., Fernandez-Zapico, M. E., Billadeau, D. D., Machius, M., Tomchick, D. R., and Rosen, M. K. (2010) Structural and energetic mechanisms of cooperative autoinhibition and activation of Vav1. *Cell* **140,** 246–256
39. Fanzo, J. C., Yang, W., Jang, S. Y., Gupta, S., Chen, Q., Siddiq, A., Greenberg, S., and Pernis, A. B. (2006) Loss of IRF-4-biding protein leads to the spontaneous development of systemic autoimmunity. *J. Clin. Invest.* **116,** 703–714
40. Altman, A., and Bécart, S. (2009) Does Def6 deficiency cause autoimmunity? *Immunity* **31,** 1–2
41. Tybulewicz, V. L., and Henderson, R. B. (2009) Rho family GTPases and their regulators in lymphocytes. *Nat. Rev. Immunol.* **9,** 630–644
42. Blomberg, K. E., Boucheron, N., Lindvall, J. M., Yu, L., Raberger, J., Berglöf, A., Ellmeier, W., and Smith, C. E. (2009) Transcriptional signatures of Itk-deficient CD3+, CD4+ and CD8+ T-cells. *BMC Genomics* **10,** 233
43. Liu, K. Q., Bunnell, S. C., Gurniak, C. B., and Berg, L. J. (1998) T cell receptor-initiated calcium release is uncoupled from capacitative calcium entry in Itk-deficient T cells. *J. Exp. Med.* **187,** 1721–1727
44. Finkelstein, L. D., Shimizu, Y., and Schwartzberg, P. L. (2005) Tec kinases regulate TCR-mediated recruitment of signaling molecules and integrin-dependent cell adhesion. *J. Immunol.* **175,** 5923–5930
45. Gomez-Rodriguez, J., Readinger, J. A., Viorritto, I. C., Mueller, K. L., Houghtling, R. A., and Schwartzberg, P. L. (2007) Tec kinases, actin, and cell adhesion. *Immunol. Rev.* **218,** 45–64
46. Dombroski, D., Houghtling, R. A., Labno, C. M., Precht, P., Takesono, A., Caplen, N. J., Billadeau, D. D., Wange, R. L., Burkhardt, J. K., and Schwartzberg, P. L. (2005) Kinase-independent functions for Itk in TCR-induced regulation of Vav and the actin cytoskeleton. *J. Immunol.* **174,** 1385–1392
47. Joseph, R. E., Min, L., and Andreotti, A. H. (2007) The linker between SH2 and kinase domains positively regulates catalysis of the Tec family kinases. *Biochemistry* **46,** 5455–5462
48. Alberti, S., Halfmann, R., King, O., Kapila, A., and Lindquist, S. (2009) A systematic survey identifies prions and illuminates sequence features of prionogenic proteins. *Cell* **137,** 146–158
49. Wickner, R. B., Edskes, H. K., Shewmaker, F., and Nakayashiki, T. (2007) Prions of fungi: inherited structures and biological roles. *Nat. Rev. Microbiol.* **5,** 611–618
50. Hao, S., and Baltimore, D. (2009) The stability of mRNA influences the temporal order of the induction of genes encoding inflammatory molecules. *Nat. Immunol.* **10,** 281–288
51. Steinmetz, M. O., Jelesarov, I., Matousek, W. M., Honnappa, S., Jahnke, W., Missimer, J. H., Frank, S., Alexandrescu, A. T., and Kammerer, R. A. (2007) Molecular basis of coiled-coil formation. *Proc. Natl. Acad. Sci. U.S.A.* **104,** 7062–7067
52. Gilks, N., Kedersha, N., Ayodele, M., Shen, L., Stoecklin, G., Dember, L. M., and Anderson, P. (2004) Stress granule assembly is mediated by prion-like aggregation of TIA-1. *Mol. Biol. Cell* **15,** 5383–5398
53. Reijns, M. A., Alexander, R. D., Spiller, M. P., and Beggs, J. D. (2008) A role for Q/N-rich aggregation-prone regions in P-body localization. *J. Cell Sci.* **121,** 2463–2472